IL NUOVO CIMENTO **39 C** (2016) 217
DOI 10.1393/ncc/i2016-16217-x

COLLOQUIA: IFAE 2015

Search for long-lived neutral particle decays using the full statistic collected in Run I with the ATLAS detector at the LHC

M. VERDUCCI

Dipartimento di Fisica, Università di Roma - Roma, Italy

received 7 January 2016

Summary. — Many extensions of the Standard Model (SM) include neutral weakly coupled particles that can be long-lived. These long-lived particles occur in many models, included gauge-mediated extensions of the Minimal Supersymmetric Model (MSSM), MSSM with R-parity violation, inelastic dark matter and the Hidden Valley (HV) scenario. Results are presented on ATLAS searches at the LHC for scalar boson decays (including rare Higgs boson decays) to pair of neutral, long-lived hidden-sector particles that lead to final states containing fermion anti-fermion pairs or pairs of collimated lepton jets. No excess of events above the expected background has been observed for $20.3\,\mathrm{fb}^{-1}$ of data collected in 2012 at a center of mass energy of 8 TeV. Limits are presented as a function of the proper lifetime of the long-lived neutral particle.

1. – Introduction

The discovery of the Higgs boson [1-3] by the ATLAS and CMS experiments [4, 5] in 2012 identified the last piece of the highly successful Standard Model (SM). Subsequent measurements of the Higgs boson branching ratios and couplings, while consistent with the SM expectations, allow for a substantial branching ratio to exotic particles. A number of extensions of the SM involve a hidden sector that is weakly coupled to the SM, with the two connected via a communicator particle.

In the so-called "CalRatio Analysis", the benchmark model is represented by the Hidden Valley (HV) models [6, 7], a general class of models that predict neutral, weakly coupled particles that can have long lifetimes (LLP). The communicator is chosen to be a SM-sector scalar boson, Φ [6-9] and it mixes with a hidden-sector scalar boson, Φ_{hs}, which decays into detectable SM particles. This search considers communicator masses between 100 GeV and 900 GeV. A Φ mass close to the mass of the discovered Higgs boson is included to search for exotic decays of the Higgs boson. The lightest HV particles form an isospin triplet of pseudoscalar particles which are called valley pions (π_{v}) because of their similarity to the SM triplet. The π_{v} are pair-produced ($\Phi_{\mathrm{hs}} \to \pi_{\mathrm{v}}\pi_{\mathrm{v}}$) and each

decays to a pair of SM fermions. The $\pi_{\rm v}$ possess Yukawa couplings to fermions and therefore preferentially decay to accessible heavy fermions, primarily $b\bar{b}$, $c\bar{c}$ and $\tau^+\tau^-$. The lifetime of the $\pi_{\rm v}$ is unconstrained and could be quite long. HV signal events are then characterised by a non-conventional detector signature: neutral vertices that can be displaced macroscopically far from the interaction point (IP). Such signatures are a challenge for trigger, detector operations, and analysis.

The analysis presented is focused on $\pi_{\rm v}$ decaying in the ATLAS hadronic calorimeter (HCal). The event topology is defined by a large deposit most of energy in HCal and very little or none in the electromagnetic calorimeter, and also have few or no charged tracks pointing at the hadronic energy deposits.

LLP are also predicted by models where the hidden sector couples with the SM via a vector portal, in which a light hidden photon (dark photon, γ_d) mixes kinetically with the SM photon. If the hidden photon is the lightest state in the hidden sector, it decays back to SM particles with branching fractions that depend on its mass [10-12]. Due to their small mass, these particles are typically produced with a large boost and, due to their weak interactions, can have non-negligible lifetime. As a result one may expect, from dark photon decays, collimated jet-like structures containing pairs of electrons and/or muons and/or charged pions ("lepton jets", LJs) that can be produced far from the primary interaction vertex of the event (displaced LJs). Since the structure of the unknown hidden sector may greatly influence the properties of the LJ, a simplified-model approach is highly beneficial. The two Falkowski-Ruderman-Volansky-Zupan (FRVZ) models [12,13], which predict non-SM Higgs boson decays to LJs are considered. For the case in which the γ_d kinetically mixes with hypercharge, one finds that ϵ, the kinetic mixing parameter, controls both the γ_d decay branching fractions and lifetime. More generally, however, the branching fractions and lifetime are model-dependent and may depend on additional parameters.

In this analysis, the LJ signals are characterised by two muons in the muon spectrometer when the γ_d decays to a muon pair or one/two jets in the calorimeters when the γ_d decays to electron/pion pair.

2. – The ATLAS experiment

The ATLAS detector [14] is a multi-purpose detector at the LHC, consisting of several sub-detectors. From the interaction point (IP) outwards there are an inner detector (ID), electromagnetic and hadronic calorimeters, and a muon spectrometer (MS). The ID, immersed in a 2 T axial magnetic field, provides tracking and vertex information for charged particles within the pseudorapidity ([1]) (η) region $|\eta| < 2.5$. It consists of three different tracking detectors. From small radii outwards, these are a silicon pixel detector, a silicon microstrip tracker (SCT) and a transition radiation tracker (TRT).

The calorimeter provides coverage over the range $|\eta| < 4.9$. It consists of a lead/liquid-argon electromagnetic calorimeter (ECal) at smaller radii ($1.5\,\text{m} < r < 2.0\,\text{m}$ in the barrel and $3.6\,\text{m} < |z| < 4.25\,\text{m}$ in the endcaps) surrounded by a hadronic calorimeter (HCal)

([1]) ATLAS uses a right-handed coordinate system with its origin at the nominal interaction point (IP) in the centre of the detector and the z-axis along the beam pipe. The x-axis points from the IP to the centre of the LHC ring, and the y-axis points upward. Cylindrical coordinates (r, ϕ) are used in the transverse plane, ϕ being the azimuthal angle around the beam pipe. The pseudorapidity is defined in terms of the polar angle θ as $\eta = -\ln\tan(\theta/2)$.

at larger radii ($2.25\,\mathrm{m} < r < 4.25\,\mathrm{m}$ in the barrel and $4.3\,\mathrm{m} < |z| < 6.05\,\mathrm{m}$ in the endcaps) comprising a steel and scintillator-tile system in the barrel region ($|\eta| < 1.7$) and a liquid-argon system with copper absorbers in the endcaps ($1.5 < |\eta| < 3.2$). Muon identification and momentum measurement are provided by the MS, which extends to $|\eta| = 2.7$. It consists of a three-layer system of gas-filled precision-tracking chambers. The region $|\eta| < 2.4$ is also covered by separate trigger chambers. A sequential three-level trigger system selects events to be recorded for offline analysis.

3. – Analysis strategy

Both the analysis presented required a signature-driven trigger that optimises the acceptance for this class of events is used for the online selection. The events selection starts with common requirements to identify collisions events with high quality detector performance.

The jets are reconstructed with an anti-k_t algorithm with $R = 0.4$ and calibrated using the local cluster weighting method [15, 16]. Jets are rejected if they do not satisfy the standard ATLAS good-jet criteria with the exception of requirements that reject jets with small electromagnetic energy fraction (EMF) [17]. Additionally, a cut on the jet timing is applied to reduce cosmic rays and beam-halo interactions backgrounds. The timing of each jet is required to satisfy $-1 < t < 5\,\mathrm{ns}$. Background processes for all the models illustrated are dominated by QCD dijet production and non-collisions background.

3˙1. *CalRatio analysis*. – Candidate events are collected using a dedicated trigger, called the *CalRatio* trigger [18], which looks specifically for long-lived neutral particles that decay near the outer radius of the ECal or within the HCal. The trigger is tuned to look for events containing at least one narrow jet with little energy deposited in the ECal and no charged tracks pointing towards the jet.

Events are rejected if any reconstructed jets show evidence of being caused by a beam-halo interaction [18]. At the level of event selection, after the common requirements due to the event quality, a cut on the missing transverse momentum is required, $E_{\mathrm{T}}^{\mathrm{miss}} < 50\,\mathrm{GeV}$, to reject non-collision events, such as cosmic rays or beam-halo interactions. One jet must have fired the CalRatio trigger. The jet matching the trigger must pass an $E_{\mathrm{T}} > 60\,\mathrm{GeV}$ requirement while a second jet must satisfy an $E_{\mathrm{T}} > 40\,\mathrm{GeV}$ requirement. If more than one jet fired the $\log_{10}(E_{\mathrm{H}}/E_{\mathrm{EM}})$ trigger then only the leading jet is required to have $E_{\mathrm{T}} > 60\,\mathrm{GeV}$. Individually, all jets must satisfy $|\eta| < 2.5$, have $\log_{10}(E_{\mathrm{H}}/E_{\mathrm{EM}}) > 1.2$, where $E_{\mathrm{H}}/E_{\mathrm{EM}}$ is the ratio of the energy deposited in the HCal (E_{H}) to the energy deposited in the ECal (E_{EM}), and have no good tracks ([2]) in the ID with $p_{\mathrm{T}} > 1\,\mathrm{GeV}$ in a region $\Delta R < 0.2$ ([3]) centred on the jet axis.

The analysis requires that exactly two jets satisfy these requirements. The second jet requirement significantly reduces the SM multi-jet background contribution.

The largest contribution to the expected background comes from SM multi-jet events. Cosmic-ray interactions contribute at a much lower level, and beam-halo interactions make a negligible contribution. To estimate the multi-jet background contribution, a

([2]) A good track must have at least two hits in the pixel detector and a total of at least nine hits in the pixel and SCT detectors.
([3]) $\Delta R = \sqrt{(\Delta\eta)^2 + (\Delta\phi)^2}$.

TABLE I. – *Requirements for selection of events with LJs. The requirements are applied to all LJ types unless otherwise specified.*

Requirement	Description
Two reconstructed LJs	select events with at least two reconstructed LJs
η range (TYPE1)	remove jets with $\|\eta\| > 2.5$
η range (TYPE2)	remove jets with $\|\eta\| > 2.5$ and $1.0 < \|\eta\| < 1.4$
EM fraction (TYPE2)	require EM fraction of the jet < 0.1
Jet Width W (TYPE2)	require width of the jet < 0.1
Jet timing (TYPE1/TYPE2)	require jets with timing $-1\,\text{ns} < t < 5\,\text{ns}$
NC muons (TYPE0/TYPE1)	require muons without ID track match
ID isolation	require $\max\{\sum p_{\text{T}}\} \leq 3\,\text{GeV}$
$\Delta\phi$	require $\|\Delta\phi| \geq 1\,\text{rad}$ between the two LJs

multi-jet data sample is used to derive the probability that a jet passes the trigger and analysis selection.

3˙2. *Lepton-jets analysis.* – The MC studies of the detector's response to the LJs guide the characterisation of the LJ and the identification of variables useful for the selection of the signal. At the detector level, a γ_d decaying to a muon pair is identified by two muons in the MS and defined as TYPE0, while a γ_d decaying to an electron/pion pair is seen as one or two jets in the calorimeters and defined as TYPE2. A cluster of two muons and one or two jets is typical of an LJ with one γ_d decaying into a muon pair and

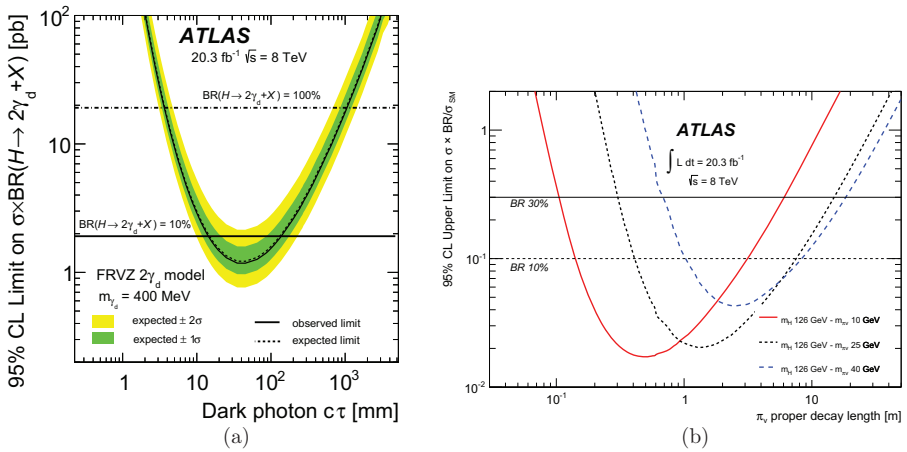

Fig. 1. – (a) The 95% upper limits on the σxBR for the processes $H \to 2\gamma_d + X$ as a function of the γ_d lifetime ($c\tau$) for the FRVZ benchmark samples, excluding the TYPE2-TYPE2 events. The expected limit is shown as the dashed curve and the almost identical solid curve shows the observed limit. The horizontal lines correspond to σxBR for two values of the BR of the Higgs boson decay to dark photons. (b) Observed 95% CL limits on $\sigma/\sigma_{\text{SM}}$ for $m_H = 126\,\text{GeV}$ as a function of the π_{v} proper decay length: the solid line is for $m_{\pi_{\text{v}}} = 10\,\text{GeV}$, the dashed line is for $m_{\pi_{\text{v}}} = 25\,\text{GeV}$, the dotted line is for $m_{\pi_{\text{v}}} = 40\,\text{GeV}$. Assuming $\sigma_{\text{SM}} = 19.0\,\text{pb}$, the horizontal solid line corresponds to BR = 30% and the horizontal dashed line to BR = 10%.

one γ_d decaying into an electron/pion pair is defined as TYPE1. The complete list of the criteria for the selection of events with different LJs TYPE is summarised in table I. The largest contribution to the expected background comes from SM multi-jet events, its evaluation is done using a data-driven (ABCD) method.

4. – Conclusions and results

The analysis presented are based on $20.3\,\mathrm{fb}^{-1}$ of pp collisions at $\sqrt{s} = 8\,\mathrm{TeV}$ collected in 2012 by the ATLAS experiment at the LHC. The observed data are consistent with the experimental background expectations. Limits are set on π_v and γ_d proper decay lengths for different scalar boson and π_v/γ_d mass combinations.

For a SM Higgs decaying to π_v proper decay lengths between 0.10 m and 18.50 m assuming a 30% BR are ruled out, and between 0.14 m and 8.32 m assuming a BR of 10%, at 95% CL. Results for low mass Φ (100 GeV and 140 GeV) and high mass Φ (300 GeV, 600 GeV, and 900 GeV) have also been estimated as a function of proper decay length.

For non-SM Higgs boson decaying to LJs according to the FRVZ models, limits are set on the σxBR for $H \to 2\gamma_d + X$ and $H \to 4\gamma_d + X$ for $\mathrm{m}_H = 125\,\mathrm{GeV}$ and a γ_d mass of 0.4 GeV. Assuming the SM gluon fusion production cross section for a 125 GeV Higgs boson, its BR to hidden-sector photons is found to be below 10%, at 95% CL, for the hidden photon γ_d in the range $14\,\mathrm{mm} < c\tau < 140\,\mathrm{mm}$ for the $2\gamma_d$ model and in the range $15\,\mathrm{mm} < c\tau < 260\,\mathrm{mm}$ for the $4\gamma_d$ model. These results are also interpreted in the context of the vector portal model as exclusion contours in the kinetic mixing parameter ϵ *vs.* γ_d Mass plane and significantly improve the constraints from other experiments (fig. 1).

REFERENCES

[1] Englert F. and Brout R., *Phys. Rev. Lett.*, **13** (1964) 321.
[2] Higgs P., *Phys. Lett.*, **12** (1964) 132.
[3] Guralnik G. S., Hagen C. R. and Kibble T. W. B., *Phys. Rev. Lett.*, **13** (1964) 585.
[4] ATLAS Collaboration, *Phys. Lett. B*, **716** (2012) 1.
[5] CMS Collaboration, *Phys. Lett. B*, **716** (2012) 30.
[6] Strassler M. J. and Zurek K. M., *Phys. Lett. B*, **651** (2007) 374–379.
[7] Strassler M. J. and Zurek K. M., *Phys. Lett. B*, **661** (2008) 263–267.
[8] Chang S., Fox P. J. and Weiner N., *JHEP*, **0608** (2006) 068.
[9] Chang S., Dermisek R., Gunion J. F. and Weiner N., *Ann. Rev. Nucl. Part. Sci.*, **58** (2008) 75-98.
[10] Falkowski A., Ruderman J. T., Volansky T. and Zupan J., *JHEP*, **05** (2010) 077.
[11] Cheung C., Ruderman J. T., Wang L.-T. and Yavin I., *Phys. Rev. D*, **80** (2009) 035008.
[12] Meade P., Papucci M. and Volansky T., *JHEP*, **12** (2009) 052.
[13] Falkowski A., Ruderman J. T., Volansky T. and Zupan J., *Phys. Rev. Lett.*, **105** (2010) 241801.
[14] ATLAS Collaboration, *JINST*, **3** (2008) S08003.
[15] Cacciari M., Salam G. P. and Soyez G., *JHEP*, **0804** (2008) 0633.
[16] ATLAS Collaboration, *Eur. Phys. J. C*, **73** (2013) 2304.
[17] ATLAS Collaboration, ATLAS-CONF-2010-038.
[18] ATLAS Collaboration, *JINST*, **8** (2013) P07015.